

Received 10 March 2020
Accepted 29 March 2020

Edited by A. J. Lough, University of Toronto,
Canada

Keywords: crystal structure; perimidin; methoxyphenol; Hirshfeld surface.

CCDC reference: 1976883

Supporting information: this article has supporting information at journals.iucr.org/e

Crystal structure, Hirshfeld surface analysis and interaction energy and DFT studies of 2-(2,3-di-hydro-1H-perimidin-2-yl)-6-methoxyphenol

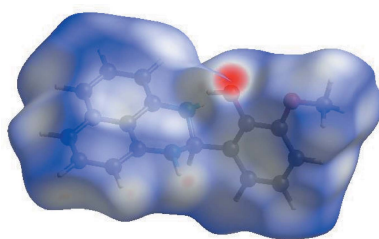
Ballo Daouda,^{a,b*} Nanou Tiéba Tuo,^b Tuncer Hökelek,^c Kangah Niameke Jean-Baptiste,^d Kodjo Charles Guillaume,^e Kablan Ahmont Landry Claude^f and El Mokhtar Essassi^a

^aLaboratoire de Chimie Organique Hétérocyclique URAC 21, Pôle de Compétence Pharmacochimie, Faculté des Sciences, Université Mohammed V, Rabat, Morocco, ^bLaboratoire de Chimie Organique et de Substances Naturelles, UFR Sciences des Structures de la Matière et Technologie, Université Félix Houphouët-Boigny, 22 BP 582 Abidjan, Côte d'Ivoire, ^cDepartment of Physics, Hacettepe University, 06800 Beytepe, Ankara, Turkey, ^dLaboratoire de Thermodynamique et Physicochimie du Milieu, Université Nangui Abrogoua, UFR-SFA, 02 BP 801 Abidjan 02, Côte d'Ivoire, ^eLaboratoire de Cristallographie et Physique Moléculaire, UFR SSMT, Université Félix Houphouët Boigny, 01 BP V34 Abidjan 01, Côte d'Ivoire, and ^fUFR des Sciences Biologiques, Université Péléforo Gon Coulibaly, BP 1328 Korhogo, Côte d'Ivoire. *Correspondence e-mail: daoudaballo526@gmail.com

The title compound, $C_{18}H_{16}N_2O_2$, consists of perimidine and methoxyphenol units, where the tricyclic perimidine unit contains a naphthalene ring system and a non-planar C_4N_2 ring adopting an envelope conformation with the NCN group hinged by $47.44(7)^\circ$ with respect to the best plane of the other five atoms. In the crystal, $O-H_{Phnl}\cdots N_{Prmdn}$ and $N-H_{Prmdn}\cdots O_{Phnl}$ ($Phnl$ = phenol and $Prmdn$ = perimidine) hydrogen bonds link the molecules into infinite chains along the *b*-axis direction. Weak $C-H\cdots \pi$ interactions may further stabilize the crystal structure. The Hirshfeld surface analysis of the crystal structure indicates that the most important contributions for the crystal packing are from $H\cdots H$ (49.0%), $H\cdots C/C\cdots H$ (35.8%) and $H\cdots O/O\cdots H$ (12.0%) interactions. Hydrogen bonding and van der Waals interactions are the dominant interactions in the crystal packing. Computational chemistry indicates that in the crystal, the $O-H_{Phnl}\cdots N_{Prmdn}$ and $N-H_{Prmdn}\cdots O_{Phnl}$ hydrogen-bond energies are 58.4 and 38.0 kJ mol^{-1} , respectively. Density functional theory (DFT) optimized structures at the B3LYP/ 6–311 G(d,p) level are compared with the experimentally determined molecular structure in the solid state. The HOMO–LUMO behaviour was elucidated to determine the energy gap.

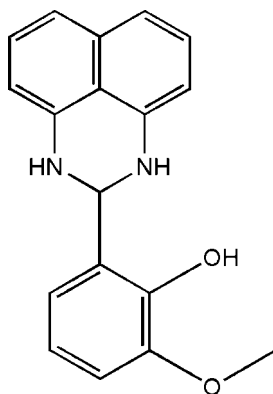
1. Chemical context

Six-membered heterocyclic compounds carrying two nitrogen atoms have been widely studied (Aly & El-Shaieb, 2004; Koca *et al.*, 2012; Zhao *et al.*, 2012; Baranov & Fadeev, 2016; Lahmadi *et al.*, 2018). Perimidine derivatives (perinaphtho-fused perimidine ring systems) in particular have aroused a lot of interest because of their applications in photophysics (Del Valle *et al.*, 1997) and their use as colouring matters for polyester fibers (Claramunt *et al.*, 1995) and as fluorescent materials (Varsha *et al.*, 2010). These molecules have a wide range of biological applications (Dzieduszycka *et al.*, 2002), indicating that the perimidine group is a potentially useful model in medicinal chemistry research and therapeutic applications. In coordination chemistry, perimidine derivatives have been studied for their interesting catalytic activities (Cucciolito *et al.*, 2013a; Akinci *et al.*, 2014) as well as in the field of corrosion inhibition (He *et al.*, 2018). As a continuation



OPEN ACCESS

of our research on the development of new perimidine derivatives with potential pharmacological applications, we studied the condensation reaction of *ortho*-vanillin and 1,8-diaminonaphthalene in ether under agitation at room temperature, which gave the title compound, 2-(2,3-dihydro-1*H*-perimidin-2-yl)-6-methoxyphenol, in good yield. We report herein the synthesis, the molecular and crystal structures along with Hirshfeld surface analysis and computational calculations of the title compound, (I).



2. Structural commentary

The title compound, (I), consists of perimidine and methoxyphenol units, where the tricyclic perimidine unit contains a naphthalene ring system and a non-planar C_4N_2 ring (Fig. 1). A puckering analysis of the non-planar six-membered C_4N_2 , *B* (N1/N2/C1/C9–C11), ring gave the parameters $q_2 = 0.3879 (12)$ Å, $q_3 = -0.2565 (12)$ Å, $Q_T = 0.4650 (13)$ Å, $\theta_2 = 123.47 (15)$ ° and $\varphi_2 = 235.98 (18)$ °]. The ring adopts an envelope conformation, where atom C1 is at the flap position and at a distance of 0.6454 (12) Å from the best plane through the other five atoms. The C_4N_2 ring is hinged about the N···N vector with the N1–C1–N2 plane being inclined by 47.44 (7)° to the best plane of the other five atoms (N1/N2/C9–C11). In the methoxyphenol moiety, the C8–O2–C4–C5 and C8–O2–C4–C3 torsion angles are $-2.9 (2)$ ° and $176.72 (12)$ °, respectively. Rings *A* (C2–C7), *C* (C10–C15) and

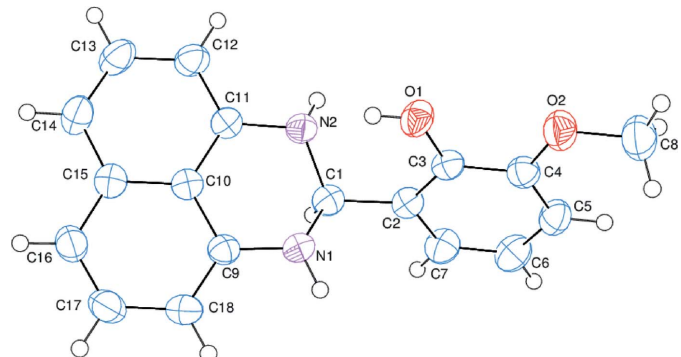


Figure 1

The asymmetric unit of the title compound with the atom-numbering scheme. Displacement ellipsoids are drawn at the 50% probability level.

Table 1
Hydrogen-bond geometry (Å, °).

Cg1 and *Cg4* are the centroids of rings *A* (C2–C7) and *D* (C9/C10/C15–C18), respectively.

<i>D</i> –H··· <i>A</i>	<i>D</i> –H	H··· <i>A</i>	<i>D</i> ··· <i>A</i>	<i>D</i> –H··· <i>A</i>
O1–H1O···N2 ⁱ	0.82	1.96	2.6667 (14)	144
N2–H2N···O1 ⁱ	0.864 (15)	2.196 (15)	2.9870 (14)	152.2 (13)
C8–H8A··· <i>Cg1</i> ^{iv}	0.96	2.82	3.6580 (17)	146
C13–H13··· <i>Cg4</i> ⁱⁱ	0.93	2.87	3.7336 (16)	155
C16–H16··· <i>Cg1</i> ^v	0.93	2.87	3.4880 (15)	125

Symmetry codes: (i) $-x + \frac{3}{2}, y + \frac{1}{2}, z$; (iv) $x, -y - \frac{1}{2}, z - \frac{1}{2}$; (v) $x + \frac{1}{2}, -y - \frac{1}{2}, -z$.

D (C9/C10/C15–C18) are oriented at dihedral angles of *A/C* = 65.39 (4)°, *A/D* = 69.63 (4)° and *C/D* = 4.31 (3)°.

3. Supramolecular features

In the crystal, O–H_{Phnl}···N_{Prmdn} and N–H_{Prmdn}···O_{Phnl} (Phnl = phenol and Prmdn = perimidine) hydrogen bonds (Table 1) link the molecules into infinite chains along the *b*-axis direction (Fig. 2). The C–H···π interactions (Table 1) may further stabilize the crystal structure.

4. Hirshfeld surface analysis

In order to visualize the intermolecular interactions in the crystal of the title compound, a Hirshfeld surface (HS) analysis (Hirshfeld, 1977; Spackman & Jayatilaka, 2009) was carried out by using *Crystal Explorer* 17.5 (Turner *et al.*, 2017). In the HS plotted over *d*_{norm} (Fig. 3), the white surface indicates contacts with distances equal to the sum of van der Waals radii, and the red and blue colours indicate distances shorter (in close contact) or longer (distinct contact) than the van der Waals radii, respectively (Venkatesan *et al.*, 2016). The bright-red spot appearing near O1 indicates its role as the respective

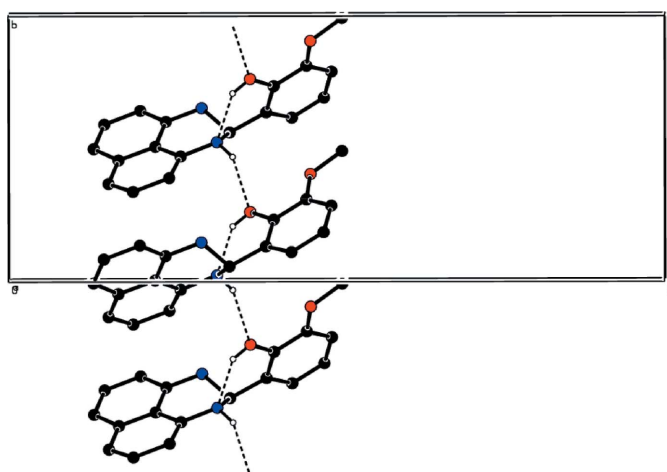
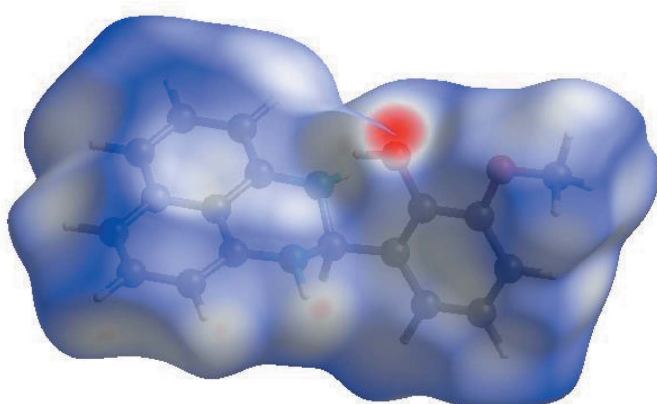


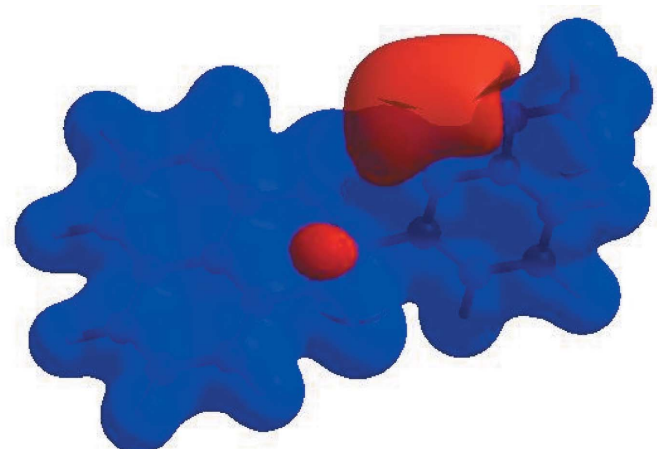
Figure 2

A partial packing diagram viewed along the *a*-axis direction with O–H_{Phnl}···N_{Prmdn} and N–H_{Prmdn}···O_{Phnl} (Phnl = phenol and Prmdn = perimidine) hydrogen bonds shown as dashed lines. H-atoms not included in hydrogen bonding have been omitted for clarity.

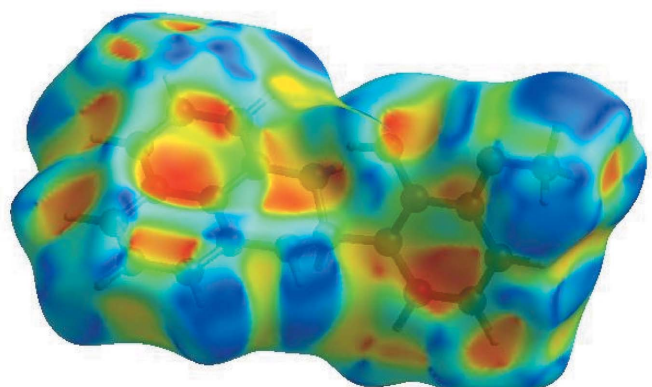
**Figure 3**

View of the three-dimensional Hirshfeld surface of the title compound plotted over d_{norm} in the range -0.4133 to 1.3883 a.u.

donor and/or acceptor; it also appears as blue and red regions corresponding to positive and negative potentials on the HS

**Figure 4**

View of the three-dimensional Hirshfeld surface of the title compound plotted over electrostatic potential energy in the range -0.0500 to 0.0500 a.u. using the STO-3G basis set at the Hartree-Fock level of theory. Hydrogen-bond donors and acceptors are shown as blue and red regions around the atoms corresponding to positive and negative potentials, respectively.

**Figure 5**

Hirshfeld surface of the title compound plotted over shape-index.

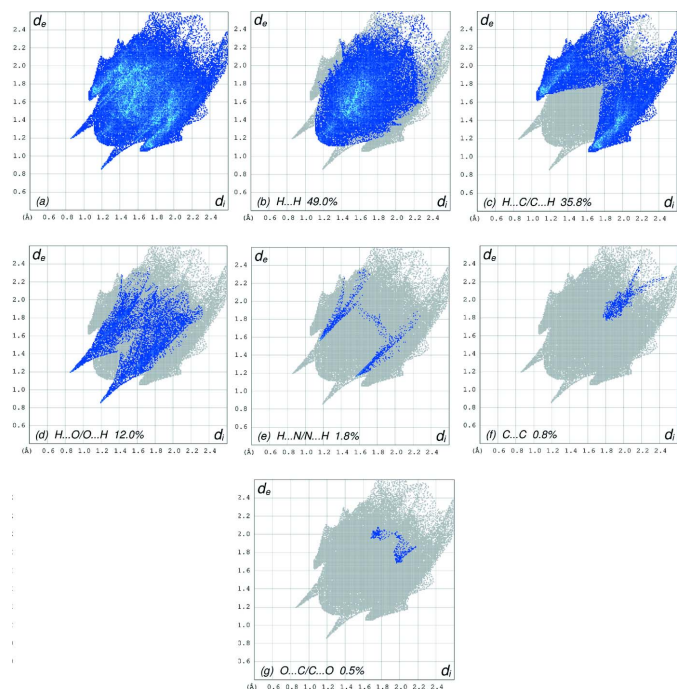
Table 2
Selected interatomic distances (\AA).

O1 \cdots O2	2.5772 (14)	C5 \cdots H8A ⁱ	2.94
O1 \cdots N2	2.6668 (14)	C5 \cdots H8B	2.72
C12 \cdots O1 ⁱ	3.1736 (17)	C5 \cdots H8C	2.80
C17 \cdots O1 ⁱⁱ	3.3145 (17)	C8 \cdots H5	2.55
C11 \cdots O1 ⁱ	3.3650 (15)	H13 \cdots C9 ⁱ	2.93
N2 \cdots O1 ⁱ	2.9867 (14)	H13 \cdots C10 ⁱ	2.97
H2N \cdots O1 ⁱ	2.196 (15)	C10 \cdots H1	2.95
H18 \cdots O1 ⁱⁱ	2.88	C12 \cdots H1O ⁱ	2.88
H12 \cdots O1 ⁱ	2.66	H1 \cdots H7	2.39
H17 \cdots O1 ⁱⁱ	2.63	H1N \cdots H18	2.44
O2 \cdots H6 ⁱⁱⁱ	2.87	H1O \cdots H2N	2.31
N1 \cdots H1O	2.86	H17 \cdots H1O ⁱⁱ	2.57
H12 \cdots N1 ⁱ	2.86	H18 \cdots H1O ⁱⁱ	2.47
N2 \cdots H1O	1.96	H2N \cdots H12	2.43
C18 \cdots C12 ⁱⁱ	3.567 (2)	H5 \cdots H8B	2.28
C1 \cdots H1O	2.46	H5 \cdots H8C	2.40
C4 \cdots H8A ⁱ	2.92	H14 \cdots H16	2.53

Symmetry codes: (i) $-x + \frac{3}{2}, y + \frac{1}{2}, z$; (ii) $x - \frac{1}{2}, y, -z + \frac{3}{2}$; (iii) $x + \frac{1}{2}, -y + \frac{1}{2}, -z + 1$.

mapped over electrostatic potential (Spackman *et al.*, 2008; Jayatilaka *et al.*, 2005) as shown in Fig. 4. The blue regions indicate the positive electrostatic potential (hydrogen-bond donors), while the red regions indicate the negative electrostatic potential (hydrogen-bond acceptors). The shape-index of the HS is a tool to visualize the π - π stacking by the presence of adjacent red and blue triangles; if there are no adjacent red and/or blue triangles, then there are no π - π interactions. Fig. 5 clearly suggests that there are no π - π interactions in (I).

The overall two-dimensional fingerprint plot, Fig. 6*a*, and those delineated into H \cdots H, H \cdots C/C \cdots H, H \cdots O/O \cdots H,

**Figure 6**

The full two-dimensional fingerprint plots for the title compound, showing (a) all interactions, and delineated into (b) H \cdots H, (c) H \cdots C/C \cdots H, (d) H \cdots O/O \cdots H, (e) H \cdots N/N \cdots H and (f) O \cdots C/C \cdots O interactions. The d_i and d_e values are the closest internal and external distances (in \AA) from given points on the Hirshfeld surface contacts.

Table 3Comparison of selected (X-ray and DFT) geometric data (\AA , $^\circ$).

Bonds/angles	X-ray	B3LYP/6–31G(d,p)
O1–C3	1.3587 (14)	1.38948
O1–H1O ^a	0.82	0.97611
N1–C9	1.3865 (16)	1.39921
N1–C1	1.4529 (17)	1.47118
N1–H1N	0.870 (15)	0.90721
C1–N2	1.4745 (16)	1.47531
C1–C2	1.5074 (17)	1.51309
O2–C4	1.3677 (15)	1.40231
O2–C8	1.4088 (17)	1.45201
N2–C11	1.4124 (16)	1.39016
N2–H2N	0.864 (15)	0.90717
C3–O1–H1O ^a	109.5	109.04
C9–N1–C1	116.86 (10)	117.19
C9–N1–H1N	115.4 (10)	116.29
C1–N1–H1N	113.3 (10)	114.01
N1–C1–N2	106.56 (10)	106.87
N1–C1–C2	109.17 (10)	110.78
N2–C1–C2	111.38 (10)	110.82
N1–C1–H1 ^a	109.9	110.12
N2–C1–H1 ^a	109.9	109.09

Note: (a) These four entries were not refined, as they each include a constrained H atom.

H···N/N···H, C···C and O···C/C···O contacts (McKinnon *et al.*, 2007) are illustrated in Fig. 6 *b–g*, respectively, together with their relative contributions to the Hirshfeld surface. The most important interaction is H···H contributing 49.0% to the overall crystal packing, which is reflected in Fig. 6*b* as widely scattered points of high density due to the large hydrogen-atom content of the molecule with the tip at $d_e = d_i = 1.20 \text{ \AA}$. In the presence of C–H··· π interactions, the pair of characteristic wings in the fingerprint plot, Fig. 6*c*, delineated into H···C/C···H contacts (Table 2; 35.8% contribution to the HS) have the tips at $d_e + d_i = 2.68 \text{ \AA}$. The pair of spikes in the fingerprint plot delineated into H···O/O···H contacts (12.0% contribution, Fig. 6*d*) have a symmetrical distribution of points with the tips at $d_e + d_i = 3.03 \text{ \AA}$. The H···N/N···H contacts (Fig. 6*e*, 1.8% contribution) have a distribution of points with the tips at $d_e + d_i = 2.72 \text{ \AA}$. The C···C contacts (0.8%, Fig. 6*f*) have the tip at $d_e = d_i = 3.37 \text{ \AA}$. Finally, the O···C/C···O interactions make only a 0.5% contribution to the overall crystal packing.

The Hirshfeld surface representations with the function d_{norm} plotted onto the surface are shown for the H···H, H···C/C···H and H···O/O···H interactions in Fig. 7*a–c*, respectively.

The Hirshfeld surface analysis confirms the importance of H-atom contacts in establishing the packing. The large number of H···H, H···C/C···H and H···O/O···H interactions suggest that van der Waals interactions and hydrogen bonding play the major roles in the crystal packing (Hathwar *et al.*, 2015).

5. Interaction energy calculations

The intermolecular interaction energies were calculated using the CE-B3LYP/6–31G(d,p) energy model available in *Crystal*

Table 4

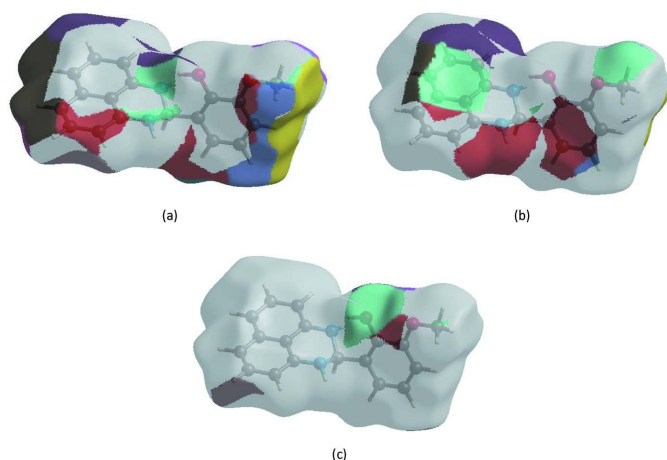
Calculated energies.

Molecular Energy (a.u.) (eV)	Compound (I)
Total Energy TE (eV)	-26013
E_{HOMO} (eV)	-3.1985
E_{LUMO} (eV)	-0.5823
Gap, ΔE (eV)	2.6162
Dipole moment, μ (Debye)	7.0880
Ionization potential, I (eV)	3.1985
Electron affinity, A	0.5823
Electronegativity, χ	1.8904
Hardness, η	1.3081
Electrophilicity index, ω	1.3660
Softness, σ	0.7645
Fraction of electrons transferred, ΔN	1.9530

(Turner *et al.*, 2017), where a cluster of molecules is generated by applying crystallographic symmetry operations with respect to a selected central molecule within a default radius of 3.8 Å (Turner *et al.*, 2014). The total intermolecular energy (E_{tot}) is the sum of electrostatic (E_{ele}), polarization (E_{pol}), dispersion (E_{dis}) and exchange-repulsion (E_{rep}) energies (Turner *et al.*, 2015) with scale factors of 1.057, 0.740, 0.871 and 0.618, respectively (Mackenzie *et al.*, 2017). Hydrogen-bonding interaction energies (in kJ mol^{-1}) were calculated as -37.5 (E_{ele}), -7.8 (E_{pol}), -52.0 (E_{dis}), 52.4 (E_{rep}) and -58.4 (E_{tot}) [or O1–H1O···N2 and -11.3 (E_{ele}), -3.4 (E_{pol}), -48.4 (E_{dis}), 30.0 (E_{rep}) and -38.0 (E_{tot}) for N2–H2N···O1].

6. DFT calculations

The optimized structure of the title compound, (I), in the gas phase was generated theoretically *via* density functional theory (DFT) using standard B3LYP functional and 6–31G(d,p) basis-set calculations (Becke, 1993) as implemented in GAUSSIAN 09 (Frisch *et al.*, 2009). The theoretical and experimental results were in good agreement (Table 3). The highest-occupied molecular orbital (HOMO), acting as an

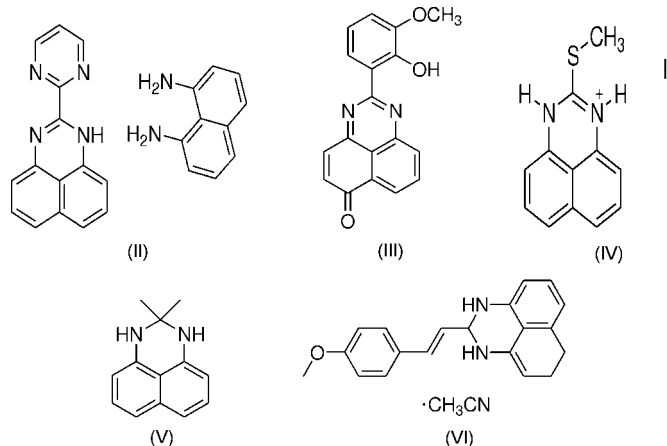
**Figure 7**

The Hirshfeld surface representations with the function d_{norm} plotted onto the surface for (a) H···H, (b) H···C/C···H and (c) H···O/O···H interactions.

electron donor, and the lowest-unoccupied molecular orbital (LUMO), acting as an electron acceptor, are very important parameters for quantum chemistry. When the energy gap is small, the molecule is highly polarizable and has high chemical reactivity. The DFT calculations provide some important information on the reactivity and site selectivity of the molecular framework. E_{HOMO} and E_{LUMO} clarify the inevitable charge-exchange collaboration inside the studied material, electronegativity (χ), hardness (η), potential (μ), electrophilicity (ω) and softness (σ) are recorded in Table 4. The significance of η and σ is for the evaluation of both the reactivity and stability. The electron transition from the HOMO to the LUMO energy level is shown in Fig. 8. The HOMO and LUMO are localized in the plane extending from the whole 2-(2,3-dihydro-1*H*-perimidin-2-yl)-6-methoxyphenol ring. The energy band gap [$\Delta E = E_{\text{LUMO}} - E_{\text{HOMO}}$] of the molecule is about 2.6162 eV, and the frontier molecular orbital energies, E_{HOMO} and E_{LUMO} are -3.1985 and -0.5823 eV, respectively.

7. Database survey

Similar compounds of the perimidine derivative have also been reported (Ghorbani, 2012; Fun *et al.*, 2011; Maloney *et al.*, 2013; Cucciolito *et al.*, 2013b; Manimekalai *et al.*, 2014), in which the groups at position 2 are almost coplanar with the perimidic nucleus (Ghorbani, 2012; Fun *et al.*, 2011; Cucciolito *et al.*, 2013b). The closest examples to the title compound, (I), are (II) (Cucciolito *et al.*, 2013b) and (III) (Fun *et al.*, 2011), while (IV) (Ghorbani, 2012), (V) (Maloney *et al.*, 2013) and (VI) (Manimekalai *et al.*, 2014) are more distant relatives.



8. Synthesis and crystallization

The title compound, (I), was synthesized from the condensation of *ortho*-vanillin (3 mmol) and 1,8-diaminonaphthalene (4 mmol) in ether (30 ml) under agitation at room temperature. Brown single crystals were obtained by the slow evaporation of the acetone solvent after 15 days (yield: 75%).

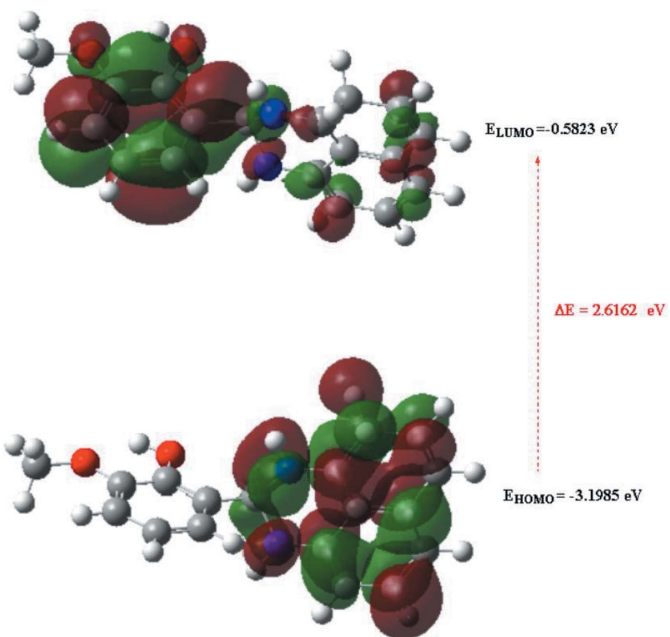


Figure 8
The energy band gap of the title compound, (I).

9. Refinement

Crystal data, data collection and structure refinement details are summarized in Table 5. The C-bound H atoms were positioned geometrically, with C—H = 0.93 Å (for aromatic H

Table 5
Experimental details.

Crystal data	
Chemical formula	C ₁₈ H ₁₆ N ₂ O ₂
M_r	292.33
Crystal system, space group	Orthorhombic, <i>Pbca</i>
Temperature (K)	293
a, b, c (Å)	12.7245 (7), 9.5887 (6), 23.7276 (14)
V (Å ³)	2895.0 (3)
Z	8
Radiation type	Mo $K\alpha$
μ (mm ⁻¹)	0.09
Crystal size (mm)	0.52 × 0.10 × 0.04
Data collection	
Diffractometer	Rigaku XtaLAB PRO
Absorption correction	Multi-scan (<i>CrysAlis PRO</i> ; Rigaku OD, 2018)
T_{\min}, T_{\max}	0.390, 1.000
No. of measured, independent and observed [$I > 2\sigma(I)$] reflections	16885, 3499, 2640
R_{int}	0.036
(sin θ/λ) _{max} (Å ⁻¹)	0.682
Refinement	
$R[F^2 > 2\sigma(F^2)], wR(F^2), S$	0.045, 0.118, 1.04
No. of reflections	3496
No. of parameters	207
H-atom treatment	H atoms treated by a mixture of independent and constrained refinement
$\Delta\rho_{\text{max}}, \Delta\rho_{\text{min}}$ (e Å ⁻³)	0.20, -0.21

Computer programs: *CrysAlis PRO* (Rigaku OD, 2018), *SHELXT* (Sheldrick, 2015a) and *SHELXL2018/3* (Sheldrick, 2015b).

atoms and H14C, H15A and H15B of the allyl moiety), 0.98 Å (for methine H atom) and 0.97 Å (for methylene H atoms), and constrained to ride on their parent atoms, with $U_{\text{iso}}(\text{H}) = 1.2U_{\text{eq}}(\text{C})$. The hydroxyl H atom was placed in a calculated position with O—H = 0.82 Å and $U_{\text{iso}}(\text{H}) = 1.5U_{\text{eq}}(\text{O})$ while H atoms bonded to N atoms were refined independently with $U_{\text{iso}}(\text{H}) = 1.2U_{\text{eq}}(\text{N})$

Funding information

TH is grateful to the Hacettepe University Scientific Research Project Unit (grant No. 013 D04 602 004).

References

- Akinci, P. A., Gülcemal, S., Kazheva, O. N., Alexandrov, G. G., Dyachenko, O. A., Çetinkaya, E. & Çetinkaya, B. (2014). *J. Organomet. Chem.* **765**, 23–30.
- Aly, A. A. & El-Shaieb, K. M. (2004). *Tetrahedron*, **60**, 3797–3802.
- Baranov, D. S. & Fadeev, D. S. (2016). *Mendeleev Commun.* **26**, 174–176.
- Becke, A. D. (1993). *J. Chem. Phys.* **98**, 5648–5652.
- Claramunt, R. M., Dotor, J. & Elguero, J. (1995). *Ann. Quim.* **91**, 151–183.
- Cucciolito, M. E., Panunzi, B., Ruffo, F. & Tuzi, A. (2013a). *Tetrahedron Lett.* **54**, 1503–1506.
- Cucciolito, M. E., Panunzi, B., Ruffo, F. & Tuzi, A. (2013b). *Acta Cryst. E69*, o1133–o1134.
- Del Valle, J. C., Catalán, J., Foces-Foces, C., Llamas-Saiz, A. L., Elguero, J., Sanz, D., Dotor, J. & Claramunt, R. M. (1997). *J. Lumin.* **75**, 17–26.
- Dzieduszycka, M., Martelli, S., Arciemiuk, M., Bontemps-Gracz, M. M., Kupiec, A. & Borowski, E. (2002). *Bioorg. Med. Chem.* **10**, 1025–1035.
- Frisch, M. J., Trucks, G. W., Schlegel, H. B., Scuseria, G. E., Robb, M. A., Cheeseman, J. R., et al. (2009). GAUSSIAN09. Gaussian Inc., Wallingford, CT, US.
- Fun, H.-K., Chanawanno, K. & Chantrapromma, S. (2011). *Acta Cryst. E67*, o715–o716.
- Ghorbani, M. H. (2012). *Acta Cryst. E68*, o2605.
- Hathwar, V. R., Sist, M., Jørgensen, M. R. V., Mamakhet, A. H., Wang, X., Hoffmann, C. M., Sugimoto, K., Overgaard, J. & Iversen, B. B. (2015). *IUCrJ*, **2**, 563–574.
- He, X., Mao, J., Ma, Q. & Tang, Y. (2018). *J. Mol. Liq.* **269**, 260–268.
- Hirshfeld, H. L. (1977). *Theor. Chim. Acta*, **44**, 129–138.
- Jayatilaka, D., Grimwood, D. J., Lee, A., Lemay, A., Russel, A. J., Taylor, C., Wolff, S. K., Cassam-Chenai, P. & Whitton, A. (2005). *TONTO - A System for Computational Chemistry*. Available at: <http://hirshfeldsurface.net/>
- Koca, I., ngren, H., Kýbrýz, E. & Yýlmaz, F. (2012). *Dyes Pigments*, **95**, 421–426.
- Lahmidi, S., Sebbar, N. K., Hökelek, T., Chkirate, K., Mague, J. T. & Essassi, E. M. (2018). *Acta Cryst. E74*, 1833–1837.
- Mackenzie, C. F., Spackman, P. R., Jayatilaka, D. & Spackman, M. A. (2017). *IUCrJ*, **4**, 575–587.
- Maloney, S., Slawin, A. M. Z. & Woollins, J. D. (2013). *Acta Cryst. E69*, o246.
- Manimekalai, A., Vijayalakshmi, N. & Selvanayagam, S. (2014). *Acta Cryst. E70*, o959.
- McKinnon, J. J., Jayatilaka, D. & Spackman, M. A. (2007). *Chem. Commun.* pp. 3814–3816.
- Rigaku OD (2018). *CrysAlis PRO*. Rigaku Oxford Diffraction, Yarnton, England.
- Sheldrick, G. M. (2015a). *Acta Cryst. A71*, 3–8.
- Sheldrick, G. M. (2015b). *Acta Cryst. C71*, 3–8.
- Spackman, M. A. & Jayatilaka, D. (2009). *CrystEngComm*, **11**, 19–32.
- Spackman, M. A., McKinnon, J. J. & Jayatilaka, D. (2008). *CrystEngComm*, **10**, 377–388.
- Turner, M. J., Grabowsky, S., Jayatilaka, D. & Spackman, M. A. (2014). *J. Phys. Chem. Lett.* **5**, 4249–4255.
- Turner, M. J., McKinnon, J. J., Wolff, S. K., Grimwood, D. J., Spackman, P. R., Jayatilaka, D. & Spackman, M. A. (2017). *CrystalExplorer17*. The University of Western Australia.
- Turner, M. J., Thomas, S. P., Shi, M. W., Jayatilaka, D. & Spackman, M. A. (2015). *Chem. Commun.* **51**, 3735–3738.
- Varsha, G., Arun, V., Robinson, P. P., Sebastian, M., Varghese, D., Leeju, P., Jayachandran, V. P. & Yusuff, K. M. M. (2010). *Tetrahedron Lett.* **51**, 2174–2177.
- Venkatesan, P., Thamotharan, S., Ilangoan, A., Liang, H. & Sundius, T. (2016). *Spectrochim. Acta Part A*, **153**, 625–636.
- Zhao, J.-F., Liu, Y., Soh, J. B., Li, Y.-X., Ganguly, R., Ye, K.-Q., Huo, F., Huang, L., Tok, A. L. Y., Loo, J. S. C. & Zhang, Q. (2012). *Tetrahedron Lett.* **53**, 6044–6047.

supporting information

Acta Cryst. (2020). E76, 605-610 [https://doi.org/10.1107/S2056989020004284]

Crystal structure, Hirshfeld surface analysis and interaction energy and DFT studies of 2-(2,3-dihydro-1*H*-perimidin-2-yl)-6-methoxyphenol

Ballo Daouda, Nanou Tiéba Tuo, Tuncer Hökelek, Kangah Niameke Jean-Baptiste, Kodjo Charles Guillaume, Kablan Ahmont Landry Claude and El Mokhtar Essassi

Computing details

Data collection: *CrysAlis PRO* (Rigaku OD, 2018); cell refinement: *CrysAlis PRO* (Rigaku OD, 2018); data reduction: *CrysAlis PRO* (Rigaku OD, 2018); program(s) used to solve structure: SHELXT (Sheldrick, 2015a); program(s) used to refine structure: *SHELXL2018/3* (Sheldrick, 2015b).

2-(2,3-Dihydro-1*H*-perimidin-2-yl)-6-methoxyphenol

Crystal data

$C_{18}H_{16}N_2O_2$
 $M_r = 292.33$
Orthorhombic, *Pbca*
 $a = 12.7245$ (7) Å
 $b = 9.5887$ (6) Å
 $c = 23.7276$ (14) Å
 $V = 2895.0$ (3) Å³
 $Z = 8$
 $F(000) = 1232$

$D_x = 1.341$ Mg m⁻³
Mo $K\alpha$ radiation, $\lambda = 0.71073$ Å
Cell parameters from 6789 reflections
 $\theta = 3.2\text{--}28.1^\circ$
 $\mu = 0.09$ mm⁻¹
 $T = 293$ K
Elongated platelet, brown
0.52 × 0.10 × 0.04 mm

Data collection

Rigaku XtaLAB PRO
diffractometer
Radiation source: micro-focus sealed X-ray
tube, Rigaku micromax 003
Rigaku Integrated Confocal MaxFlux double
bounce multi-layer mirror optics
monochromator
Detector resolution: 5.811 pixels mm⁻¹
 ω scans

Absorption correction: multi-scan
(CrysAlisPro; Rigaku OD, 2018)
 $T_{\min} = 0.390$, $T_{\max} = 1.000$
16885 measured reflections
3499 independent reflections
2640 reflections with $I > 2\sigma(I)$
 $R_{\text{int}} = 0.036$
 $\theta_{\max} = 29.0^\circ$, $\theta_{\min} = 2.4^\circ$
 $h = -16 \rightarrow 14$
 $k = -12 \rightarrow 13$
 $l = -30 \rightarrow 30$

Refinement

Refinement on F^2
Least-squares matrix: full
 $R[F^2 > 2\sigma(F^2)] = 0.045$
 $wR(F^2) = 0.118$
 $S = 1.04$
3496 reflections
207 parameters

0 restraints
Primary atom site location: other
Secondary atom site location: difference Fourier
map
Hydrogen site location: mixed
H atoms treated by a mixture of independent
and constrained refinement

$$w = 1/[\sigma^2(F_o^2) + (0.0609P)^2 + 0.4131P]$$

where $P = (F_o^2 + 2F_c^2)/3$
 $(\Delta/\sigma)_{\max} = 0.001$

$$\Delta\rho_{\max} = 0.20 \text{ e } \text{\AA}^{-3}$$

$$\Delta\rho_{\min} = -0.21 \text{ e } \text{\AA}^{-3}$$

Special details

Geometry. All esds (except the esd in the dihedral angle between two l.s. planes) are estimated using the full covariance matrix. The cell esds are taken into account individually in the estimation of esds in distances, angles and torsion angles; correlations between esds in cell parameters are only used when they are defined by crystal symmetry. An approximate (isotropic) treatment of cell esds is used for estimating esds involving l.s. planes.

Fractional atomic coordinates and isotropic or equivalent isotropic displacement parameters (\AA^2)

	<i>x</i>	<i>y</i>	<i>z</i>	$U_{\text{iso}}^*/U_{\text{eq}}$
O1	0.73352 (7)	0.23966 (10)	0.63178 (4)	0.0437 (2)
H1O	0.731483	0.294081	0.658419	0.066*
N1	0.52935 (9)	0.35194 (11)	0.70590 (5)	0.0395 (3)
H1N	0.4730 (12)	0.3089 (15)	0.6946 (6)	0.047*
C1	0.57436 (10)	0.44289 (13)	0.66329 (5)	0.0373 (3)
H1	0.532216	0.528041	0.659972	0.045*
O2	0.72915 (8)	0.09678 (11)	0.53981 (4)	0.0519 (3)
N2	0.68133 (8)	0.47793 (11)	0.68254 (4)	0.0379 (3)
H2N	0.7113 (11)	0.5331 (16)	0.6587 (6)	0.045*
C2	0.57650 (10)	0.36729 (13)	0.60760 (5)	0.0363 (3)
C3	0.65312 (9)	0.26779 (12)	0.59586 (5)	0.0346 (3)
C4	0.64940 (10)	0.19120 (13)	0.54596 (5)	0.0383 (3)
C5	0.56894 (11)	0.21405 (14)	0.50790 (6)	0.0449 (3)
H5	0.566134	0.163263	0.474546	0.054*
C6	0.49246 (11)	0.31282 (15)	0.51959 (6)	0.0500 (4)
H6	0.438253	0.327981	0.494027	0.060*
C9	0.52580 (9)	0.40296 (12)	0.76054 (5)	0.0346 (3)
C7	0.49623 (11)	0.38823 (14)	0.56858 (6)	0.0458 (3)
H7	0.444503	0.454306	0.575894	0.055*
C8	0.72720 (13)	0.01056 (17)	0.49174 (7)	0.0603 (4)
H8A	0.788077	-0.048578	0.491698	0.090*
H8B	0.727304	0.067394	0.458433	0.090*
H8C	0.664899	-0.045880	0.492341	0.090*
C10	0.60767 (9)	0.49588 (12)	0.77664 (5)	0.0335 (3)
C11	0.68804 (9)	0.53139 (12)	0.73789 (5)	0.0347 (3)
C12	0.77148 (11)	0.61181 (14)	0.75512 (6)	0.0441 (3)
H12	0.825905	0.631841	0.730241	0.053*
C13	0.77415 (12)	0.66349 (15)	0.81036 (6)	0.0506 (4)
H13	0.830410	0.718819	0.821577	0.061*
C14	0.69668 (12)	0.63475 (14)	0.84781 (6)	0.0479 (3)
H14	0.699244	0.673103	0.883784	0.057*
C15	0.61190 (10)	0.54681 (13)	0.83261 (5)	0.0384 (3)
C16	0.53296 (10)	0.50546 (15)	0.87065 (6)	0.0451 (3)
H16	0.532878	0.540825	0.907150	0.054*
C17	0.45685 (11)	0.41435 (16)	0.85456 (6)	0.0498 (4)
H17	0.406633	0.386074	0.880644	0.060*

C18	0.45257 (10)	0.36232 (15)	0.79961 (6)	0.0445 (3)
H18	0.399877	0.299926	0.789503	0.053*

Atomic displacement parameters (\AA^2)

	U^{11}	U^{22}	U^{33}	U^{12}	U^{13}	U^{23}
O1	0.0417 (5)	0.0466 (5)	0.0427 (5)	0.0082 (4)	-0.0125 (4)	-0.0068 (4)
N1	0.0352 (6)	0.0420 (6)	0.0412 (6)	-0.0088 (5)	0.0001 (4)	-0.0046 (5)
C1	0.0358 (7)	0.0346 (6)	0.0416 (7)	0.0020 (5)	-0.0025 (5)	0.0001 (5)
O2	0.0499 (6)	0.0560 (6)	0.0499 (6)	0.0108 (5)	-0.0044 (4)	-0.0146 (5)
N2	0.0378 (6)	0.0389 (6)	0.0370 (6)	-0.0084 (5)	0.0024 (4)	0.0003 (4)
C2	0.0382 (6)	0.0346 (6)	0.0361 (6)	-0.0014 (5)	-0.0029 (5)	0.0039 (5)
C3	0.0336 (6)	0.0356 (6)	0.0347 (6)	-0.0029 (5)	-0.0035 (5)	0.0048 (5)
C4	0.0380 (7)	0.0381 (6)	0.0387 (7)	-0.0015 (5)	0.0007 (5)	0.0012 (5)
C5	0.0510 (8)	0.0482 (8)	0.0354 (7)	-0.0046 (6)	-0.0051 (6)	-0.0013 (6)
C6	0.0500 (8)	0.0550 (8)	0.0451 (8)	0.0023 (7)	-0.0163 (6)	0.0049 (7)
C9	0.0309 (6)	0.0339 (6)	0.0389 (7)	0.0033 (5)	-0.0009 (5)	0.0000 (5)
C7	0.0439 (7)	0.0458 (7)	0.0476 (8)	0.0072 (6)	-0.0095 (6)	0.0021 (6)
C8	0.0658 (10)	0.0599 (10)	0.0551 (9)	0.0081 (8)	0.0010 (7)	-0.0165 (8)
C10	0.0336 (6)	0.0298 (6)	0.0372 (6)	0.0032 (5)	-0.0017 (5)	0.0027 (5)
C11	0.0371 (6)	0.0300 (6)	0.0371 (6)	-0.0005 (5)	-0.0010 (5)	0.0020 (5)
C12	0.0431 (7)	0.0437 (7)	0.0454 (7)	-0.0106 (6)	-0.0011 (6)	0.0032 (6)
C13	0.0550 (9)	0.0468 (8)	0.0499 (8)	-0.0182 (7)	-0.0099 (6)	0.0010 (7)
C14	0.0599 (9)	0.0446 (7)	0.0392 (7)	-0.0069 (7)	-0.0064 (6)	-0.0033 (6)
C15	0.0414 (7)	0.0355 (6)	0.0384 (7)	0.0047 (5)	-0.0030 (5)	0.0016 (5)
C16	0.0445 (7)	0.0547 (8)	0.0362 (7)	0.0053 (6)	0.0017 (5)	-0.0019 (6)
C17	0.0380 (7)	0.0662 (9)	0.0452 (8)	0.0001 (7)	0.0079 (6)	0.0039 (7)
C18	0.0328 (7)	0.0502 (8)	0.0504 (8)	-0.0046 (6)	0.0027 (6)	-0.0005 (6)

Geometric parameters (\AA , $^\circ$)

O1—C3	1.3587 (14)	C9—C10	1.4230 (17)
O1—H1O	0.8200	C7—H7	0.9300
N1—C9	1.3865 (16)	C8—H8A	0.9600
N1—C1	1.4529 (17)	C8—H8B	0.9600
N1—H1N	0.870 (15)	C8—H8C	0.9600
C1—N2	1.4745 (16)	C10—C15	1.4161 (17)
C1—C2	1.5074 (17)	C10—C11	1.4168 (16)
C1—H1	0.9800	C11—C12	1.3744 (18)
O2—C4	1.3677 (15)	C12—C13	1.4017 (19)
O2—C8	1.4088 (17)	C12—H12	0.9300
N2—C11	1.4124 (16)	C13—C14	1.355 (2)
N2—H2N	0.864 (15)	C13—H13	0.9300
C2—C3	1.3922 (17)	C14—C15	1.4160 (19)
C2—C7	1.3930 (17)	C14—H14	0.9300
C3—C4	1.3942 (17)	C15—C16	1.4074 (18)
C4—C5	1.3826 (18)	C16—C17	1.359 (2)
C5—C6	1.386 (2)	C16—H16	0.9300

C5—H5	0.9300	C17—C18	1.397 (2)
C6—C7	1.370 (2)	C17—H17	0.9300
C6—H6	0.9300	C18—H18	0.9300
C9—C18	1.3710 (17)		
O1···O2	2.5772 (14)	C5···H8A ⁱ	2.94
O1···N2	2.6668 (14)	C5···H8B	2.72
C12···O1 ⁱ	3.1736 (17)	C5···H8C	2.80
C17···O1 ⁱⁱ	3.3145 (17)	C8···H5	2.55
C11···O1 ⁱ	3.3650 (15)	H13···C9 ⁱ	2.93
N2···O1 ⁱ	2.9867 (14)	H13···C10 ⁱ	2.97
H2N···O1 ⁱ	2.196 (15)	C10···H1	2.95
H18···O1 ⁱⁱ	2.88	C12···H1O ⁱ	2.88
H12···O1 ⁱ	2.66	H1···H7	2.39
H17···O1 ⁱⁱ	2.63	H1N···H18	2.44
O2···H6 ⁱⁱⁱ	2.87	H1O···H2N	2.31
N1···H1O	2.86	H17···H1O ⁱⁱ	2.57
H12···N1 ⁱ	2.86	H18···H1O ⁱⁱ	2.47
N2···H1O	1.96	H2N···H12	2.43
C18···C12 ⁱⁱ	3.567 (2)	H5···H8B	2.28
C1···H1O	2.46	H5···H8C	2.40
C4···H8A ⁱ	2.92	H14···H16	2.53
C3—O1—H1O	109.5	C2—C7—H7	119.5
C9—N1—C1	116.86 (10)	O2—C8—H8A	109.5
C9—N1—H1N	115.4 (10)	O2—C8—H8B	109.5
C1—N1—H1N	113.3 (10)	H8A—C8—H8B	109.5
N1—C1—N2	106.56 (10)	O2—C8—H8C	109.5
N1—C1—C2	109.17 (10)	H8A—C8—H8C	109.5
N2—C1—C2	111.38 (10)	H8B—C8—H8C	109.5
N1—C1—H1	109.9	C15—C10—C11	119.89 (11)
N2—C1—H1	109.9	C15—C10—C9	119.70 (11)
C2—C1—H1	109.9	C11—C10—C9	120.31 (11)
C4—O2—C8	117.50 (11)	C12—C11—N2	121.79 (11)
C11—N2—C1	115.25 (10)	C12—C11—C10	119.96 (11)
C11—N2—H2N	111.1 (10)	N2—C11—C10	118.20 (10)
C1—N2—H2N	110.1 (10)	C11—C12—C13	119.68 (12)
C3—C2—C7	118.64 (12)	C11—C12—H12	120.2
C3—C2—C1	121.17 (11)	C13—C12—H12	120.2
C7—C2—C1	120.00 (11)	C14—C13—C12	121.57 (13)
O1—C3—C2	122.54 (11)	C14—C13—H13	119.2
O1—C3—C4	116.99 (11)	C12—C13—H13	119.2
C2—C3—C4	120.47 (11)	C13—C14—C15	120.54 (12)
O2—C4—C5	125.78 (12)	C13—C14—H14	119.7
O2—C4—C3	114.47 (11)	C15—C14—H14	119.7
C5—C4—C3	119.75 (12)	C16—C15—C14	123.25 (12)
C4—C5—C6	119.84 (12)	C16—C15—C10	118.50 (12)
C4—C5—H5	120.1	C14—C15—C10	118.24 (12)

C6—C5—H5	120.1	C17—C16—C15	120.63 (13)
C7—C6—C5	120.39 (12)	C17—C16—H16	119.7
C7—C6—H6	119.8	C15—C16—H16	119.7
C5—C6—H6	119.8	C16—C17—C18	121.31 (13)
C18—C9—N1	123.65 (12)	C16—C17—H17	119.3
C18—C9—C10	119.61 (12)	C18—C17—H17	119.3
N1—C9—C10	116.62 (11)	C9—C18—C17	120.20 (13)
C6—C7—C2	120.90 (13)	C9—C18—H18	119.9
C6—C7—H7	119.5	C17—C18—H18	119.9
C9—N1—C1—N2	56.76 (13)	C18—C9—C10—C15	-0.81 (17)
C9—N1—C1—C2	177.15 (10)	N1—C9—C10—C15	-176.97 (10)
N1—C1—N2—C11	-52.57 (13)	C18—C9—C10—C11	175.67 (11)
C2—C1—N2—C11	-171.54 (10)	N1—C9—C10—C11	-0.50 (16)
N1—C1—C2—C3	-78.14 (14)	C1—N2—C11—C12	-157.13 (12)
N2—C1—C2—C3	39.26 (16)	C1—N2—C11—C10	25.13 (15)
N1—C1—C2—C7	96.72 (13)	C15—C10—C11—C12	1.88 (17)
N2—C1—C2—C7	-145.88 (12)	C9—C10—C11—C12	-174.59 (11)
C7—C2—C3—O1	-179.32 (11)	C15—C10—C11—N2	179.66 (10)
C1—C2—C3—O1	-4.39 (18)	C9—C10—C11—N2	3.19 (17)
C7—C2—C3—C4	0.17 (18)	N2—C11—C12—C13	179.45 (12)
C1—C2—C3—C4	175.10 (11)	C10—C11—C12—C13	-2.86 (19)
C8—O2—C4—C5	-2.9 (2)	C11—C12—C13—C14	0.8 (2)
C8—O2—C4—C3	176.72 (12)	C12—C13—C14—C15	2.2 (2)
O1—C3—C4—O2	-0.28 (16)	C13—C14—C15—C16	175.57 (13)
C2—C3—C4—O2	-179.80 (11)	C13—C14—C15—C10	-3.1 (2)
O1—C3—C4—C5	179.39 (12)	C11—C10—C15—C16	-177.68 (11)
C2—C3—C4—C5	-0.13 (18)	C9—C10—C15—C16	-1.19 (17)
O2—C4—C5—C6	179.60 (12)	C11—C10—C15—C14	1.09 (17)
C3—C4—C5—C6	0.0 (2)	C9—C10—C15—C14	177.58 (11)
C4—C5—C6—C7	0.2 (2)	C14—C15—C16—C17	-176.13 (13)
C1—N1—C9—C18	152.51 (12)	C10—C15—C16—C17	2.57 (19)
C1—N1—C9—C10	-31.50 (15)	C15—C16—C17—C18	-2.0 (2)
C5—C6—C7—C2	-0.1 (2)	N1—C9—C18—C17	177.36 (12)
C3—C2—C7—C6	-0.1 (2)	C10—C9—C18—C17	1.5 (2)
C1—C2—C7—C6	-175.04 (13)	C16—C17—C18—C9	-0.1 (2)

Symmetry codes: (i) $-x+3/2, y+1/2, z$; (ii) $x-1/2, y, -z+3/2$; (iii) $x+1/2, -y+1/2, -z+1$.

Hydrogen-bond geometry (\AA , $^\circ$)

Cg1 and Cg4 are the centroids of rings A (C2—C7) and D (C9/C10/C15—C18), respectively.

$D\cdots H\cdots A$	$D—H$	$H\cdots A$	$D\cdots A$	$D—H\cdots A$
O1—H1O \cdots N2	0.82	1.96	2.6667 (14)	144
N2—H2N \cdots O1 ⁱ	0.864 (15)	2.196 (15)	2.9870 (14)	152.2 (13)
C8—H8A \cdots Cg1 ^{iv}	0.96	2.82	3.6580 (17)	146

C13—H13···Cg4 ⁱ	0.93	2.87	3.7336 (16)	155
C16—H16···Cg1 ^v	0.93	2.87	3.4880 (15)	125

Symmetry codes: (i) $-x+3/2, y+1/2, z$; (iv) $x, -y-1/2, z-1/2$; (v) $x+1/2, -y-1/2, -z$.